*Original Article*

Institution of MECHANICAL ENGINEERS

Journal of AUTOMOBILE ENGINEERING

*Proc IMechE Part D:*
*J Automobile Engineering*
2017, Vol. 231(4) 555–566

DOI: 10.1177/0954407016661440
journals.sagepub.com/home/pid
SAGE

# Potential of variable diffuser vanes for extending the operating range of compressors and for improving the torque performance of turbocharged engines

**Qiangqiang Huang and Xinqian Zheng**

**Abstract**

Turbocharging plays a significant role in internal-combustion engines. For engines in the future or for engines operating at a high altitude, compressors which are able to deliver a high pressure ratio are preferable. However, the poor low-end torque characteristics of turbocharged engines, which are often restricted by the narrow operating range of compressors at a high pressure ratio, result in a severe problem for turbocharging. The use of variable diffuser vanes is an effective method to increase the operating range, but the potential of an extended operating range at a high pressure ratio and improvement in the torque performance of engines is unclear. Nowadays, the pressure ratio of a turbocharger compressor may be only 1–4. Because of the increase in the pressure ratio, estimating the potential is ultimately worthwhile. In this paper the performances of a centrifugal compressor with different diffuser vane angles are investigated, the range extension and the improvement in the torque performance which benefited from variable diffuser vanes are estimated and the mechanisms for range extension are revealed. The approach includes steady three-dimensional Reynolds-averaged Navier–Stokes simulations and theoretical analysis. Adjusting the vane angle from $-10°$ to $10°$ improves the operating range of a compressor from 23.5% (with fixed vanes) to 54.9% at a pressure ratio of 4.8. The range extension is obtained by utilizing the shifts in the choke line and the surge line. A method of assessing the choking component based on the simulation results is proposed. The diffuser, the flow stability of which was enhanced comparatively by closing it (pivoting the vanes by $-10°$ and $-5°$), contributes mainly to reducing the surge flow. With this range extension, the improvement in the maximum torque is estimated to be 78%.

**Keywords**

Turbocharged engine, compressor, variable diffuser vanes, range extension, torque improvement

Date received: 24 December 2015; accepted: 10 June 2016

## Introduction

The automotive industry devotes huge efforts to develop cleaner and more economical engines. At present, in the development of gasoline engine, the major driving force is to improve the efficiency, but for diesel engines reducing the soot emissions and the nitrogen oxide ($NO_x$) emissions is needed more urgently.[1] Turbocharging, which can help to achieve both of these goals, is becoming an increasingly preferred choice. The soot emissions and the $NO_x$ emissions from diesel engines have a trade-off relation. However, in the experiments carried out by Aoyagi et al.[2, 3] and Wakisaka et al.,[4] the extremely high pressure intake facilitated simultaneously a reduction in the $NO_x$ emissions and a reduction in the soot emissions from diesel engines. For gasoline engines, the cylinder is cooler because of direct injection, which alleviates the knock tendency; this makes a higher boost pressure and further downsizing possible, and thus this combination of turbocharging and direct injection greatly

Turbomachinery Laboratory, State Key Laboratory of Automotive Safety and Energy, Tsinghua University, Beijing, People's Republic of China

**Corresponding author:**
Xinqian Zheng, Turbomachinery Laboratory, State Key Laboratory of Automotive Safety and Energy, Tsinghua University, Beijing 100084, People's Republic of China.
Email: zhengxq@tsinghua.edu.cn

benefits the efficiency of the gasoline engine.[5] Also, as variable-compression-ratio methods become more advanced, such as the Miller cycle on gasoline engines, a force-induced intake with a high pressure is desirable to compensates the volumetric efficiency.[6, 7] Turbocharging will play a significant role in the future combination of technologies for eco-friendly conventional engines. In all the scenarios for the car market in the next few decades described by Bandivadekar et al.,[8] turbocharged engines were predicted to take a market share of more than 25%.

The vast need for a high boost pressure from turbochargers drives engineers to develop advanced turbocharging technologies. A severe problem concerning turbocharging is the poor low-end torque of turbocharged engines.[9–11] At low engine shaft speeds, the air charging system of an engine works at a low mass flow rate where the compressor is likely to be involved in surge or stall and to fail to compress air stably, in particular at high pressure ratios. If the compressor cannot feed the cylinders with a high pressure intake as needed, the engine cannot produce sufficient low-end torque. Therefore, the narrow operating range (the mass flow range between surge and choke) of compressors at a high pressure ratio markedly restricts the engine performance.

Much research is concerned with widening the operating range of compressors or intake systems. Parallel or series sequential turbocharging combines a high-pressure compressor and a low-pressure compressor and then superposes both the characteristics to obtain a wide flow range.[12] This method is effective but has a high cost and requires a large space. A single turbocharger compressor also can obtain an extended range by using various methods. The techniques that have a fixed geometry after treatments include casing treatment,[13, 14] backswept blades[15] and blade trimming,[16] all of which shift the surge line of the compressors permanently. The variable-geometry method, which mainly refers to variable inlet prewhirl or variable diffuser,[17] is an alternative way to achieve different compressor characteristics by adjusting the geometry of compressors. This not only widens the operating range but also can modulate the flow to improve the efficiency in off-design conditions.

The use of variable diffuser vanes is a variable-geometry method which manipulates the vaned diffuser of a centrifugal compressor. Simon et al.[18] adjusted the vane angles of the diffuser and found that the method of variable diffuser vanes extends the operating range greatly. They even combined it with variable inlet guide vanes and achieved an additional improvement in the efficiency. Hunziker and Gyarmathy[19] employed variable diffuser vanes to investigate the influences of the characteristics of the components on the flow stability of the whole compressor and found that diffuser channels played an inherently destabilizing role. Although their work does not utilize the flow control method, it presents a lot of measurement data about the internal flow inside the diffuser with different vane angles, which can be the basis for developing variable diffuser vanes. Jiao et al.[20] validated the effectiveness of variable diffuser vanes in range extension by numerical simulations, but the peak pressure ratio of the compressor in their work is only near to 2.7. Currently, a low pressure ratio is widely applied on automotive turbocharged engines. In the future, however, as boosting technologies are developed, much higher pressure ratios are likely to be popular. Estimation of the range extension potential of variable diffuser vanes for a high-pressure-ratio compressor is necessary ultimately.

Wöhr et al.[11] predicted that variable diffuser vanes can help an engine to achieve a lower fuel consumption and better low-end torque characteristics. This study will go into detail about the compressor aerodynamics and the improvement in the torque performance obtained by using variable diffuser vanes was quantitatively estimated. The main body of this paper is divided into three parts. First, the methodology is described. Second, the compressor performances with five stagger angles of the diffuser vanes are presented. The range extension obtained by variable diffuser vanes is measured on the combined map of five stagger angles. Furthermore, the mechanism of how the stagger angle influences the operating range is explained. Finally, the improvement in the maximum torque of an engine in the extended operating range is estimated.

## Methodology for the simulations

Numeca FINE/Turbo is employed for the computational fluid dynamic simulations. The equations governing the flow are steady-state Reynolds-averaged Navier–Stokes equations. The central scheme and the fourth-order Runge–Kutta scheme were selected for spatial discretization and temporal discretization respectively. The Spalart–Allmaras one-equation model was used as the turbulence model. The rotor–stator interface was modelled by the full non-matching mixing-plane method. A similar setup for the numerical method has been applied to the open test case SRV2-O,[21, 22] which validates the fidelity of the code to represent the performances of the components and the flow features upstream of the impeller blades and the diffuser vanes.

The main parameters of the investigated compressor are listed in Table 1. The compressor has nine main-blade–splitter couples and 16 vanes in the diffuser. Only a single impeller blade passage and a single diffuser passage were meshed to construct the computational domain, and the side faces of passages were periodically matched, as shown in Figure 1(a). As shown in Figure 1(b), the diffuser vanes were turned by $\pm 5^\circ$ and $\pm 10^\circ$ to investigate the compressor performance with variable diffuser vanes. The pivot of each vane is located at the middle point of the centre line. The number of nodes in the mesh and the quality vary

**Table 1.** Compressor parameters.

| Parameter | Value for the following | | | | |
|---|---|---|---|---|---|
| | Closed 10° case | Closed 5° case | DATUM case | Open 5° case | Open 10° case |
| Area of the diffuser throat (mm$^2$) | $3.31 \times 10^2$ | $4.53 \times 10^2$ | $5.67 \times 10^2$ | $6.73 \times 10^2$ | $7.68 \times 10^2$ |
| Maximum rotational speed $N_{max}$ (r/min) | | | 111,700 | | |
| Tip radius at the impeller exit (mm) | | | 50.00 | | |
| Area of the impeller throat (mm$^2$) | | | $1.74 \times 10^3$ | | |

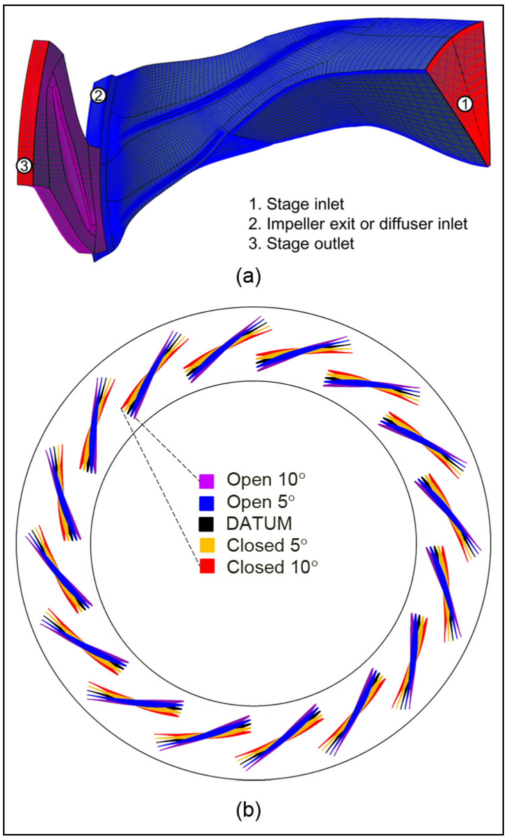


**Figure 1.** Mesh and schedule for adjusting the diffuser vanes: (a) the mesh of the DATUM compressor; (b) the diffusers with different vane angles.

little with the vane angle, so the mesh of the datum compressor is taken as representative. It has $1.05 \times 10^6$ nodes of which the impeller occupies $0.88 \times 10^6$ nodes; the minimum skewness angles in the impeller and the diffuser are 19.67° and 44.68° respectively. The mesh quality and the independence have been validated in previous work by one of the present authors and co-authors.[23] The width of the first layer of cells, namely 0.002 mm, ensures that $y^+$ is less than 10 in all simulations, which satisfies the turbulence model for resolving the viscous sublayer.[24] The shroud gap of the impeller is 0.5 mm. The stagger angle of diffuser vanes can be adjusted, so there should be a gap between the vanes and the wall. However, there is no standard about the size of the gap. The gap can be manufactured to be quite small, as it is between stationary and planar surfaces. Therefore, the clearance between the vanes and the diffuser wall was not meshed.

For the inlet boundary conditions, the velocity is normal to the inlet. It is average value at the inlet. The absolute total pressure and the total temperature are 101.325 kPa and 298.15 K respectively. Non-slip and impermeability conditions were imposed on all solid surfaces. The simulations were conducted at rotational speeds of $1.0N_{max}$, $0.9N_{max}$, $0.8N_{max}$, $0.7N_{max}$, $0.6N_{max}$ and $0.4N_{max}$ (only the datum compressor was simulated at $0.7N_{max}$). Since the peak of the pressure ratio characteristics provide a convenient engineering approximation for flow instability,[25] it is taken as the surge point. Alternatively, if the computation diverges before reaching the peak pressure ratio with decreasing mass flow rate, the operation point with the lowest mass flow that still converged is considered to be the surge point. Sometimes, flow recirculation, which is a local flow feature, is used to determine the surge point, but this may be effective for only one component. Stall in one component may not be sufficient to cause the whole stage to flow instabilities,[26] so the local flow feature is not taken as the criterion. Although, the surge line determined by the peak pressure ratio is not totally accurate; it works well to observe the change in the flow stabilities of the specific stage or the components after using the flow control method.

## Widening the operating range of a compressor

### *Performance and range extension*

Figure 2(a) shows the compressor pressure ratio characteristics with different stagger angles of the vanes. The compressor performance moves to the left via closing the diffuser vanes, and to the right via opening the diffuser vanes. At the maximum speed, the peak pressure ratio with an adjusted diffuser obviously decreases. As shown in Figure 2(b), the compressor employing variable diffuser vanes has a broader range than the datum compressor which is equipped with a fixed diffuser. The operating range of a compressor is defined as

$$\text{Operating range} = \left(1 - \frac{\dot{m}_s}{\dot{m}_c}\right)_{\pi = constant} \times 100\% \quad (1)$$

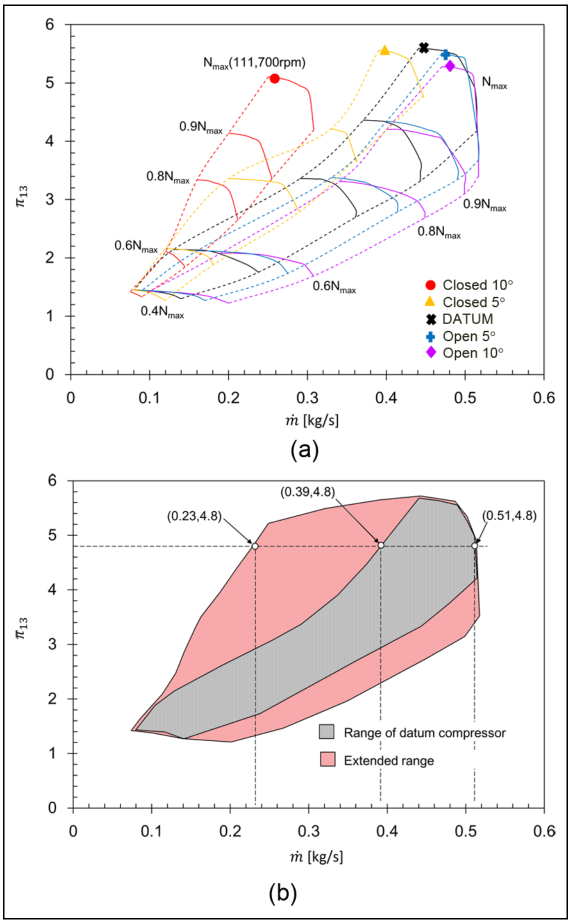


**Figure 2.** Range extensions and performances: (a) pressure ratio performances; (b) range extensions obtained by variable diffuser vanes.
rpm: r/min.

For a pressure ratio of 4.8, the operating range of the datum compressor is only 23.5% (i.e. $1 - 0.39/0.51$), and variable diffuser vanes with angles between $-10°$ and 10° increases it to 54.9%. If the clearance between the diffuser vanes and the diffuser wall is taken into account, the extended operating range can be larger.[27] In a recent research study, the operating range obtained by variable inlet prewhirl between 0° and 60° is 49% at the pressure ratio[28] of 4.8. From this we cannot conclude which method is better and, in fact, the effects of both methods depend strongly on the adjustable range of the prewhirl or the vane angle. Here we just intend to provide examples of the magnitudes of the required angle ranges of these two methods for similar range extension effects.

At a rotational speed of $N_{max}$, the shift in the surge line obtained by closing the diffuser is the main reason for widening the operating range. However, at rotational speeds of $0.9N_{max}$ and $0.8N_{max}$, the shift in the choke line obtained by opening the diffuser also has a considerable influence in extending the operating range. At rotational speeds of $0.4N_{max}$ and $0.6N_{max}$, the surge flow almost does not change after closing the diffuser. Therefore, it can be seen that the reasons controlling range extension at different speeds are different.

Although closing the diffuser results in a large range extension, the efficiency for the 'closed 10°' case decreases greatly at all speeds. As shown in Figure 3(a), the decrease in the peak efficiency in comparison with the datum compressor is 13.8% at $N_{max}$. Because of the backswept impeller, which makes the work input go up when the mass flow is decreased, the pressure ratio level with a closed diffuser does not decrease as much as the efficiency does. By contrast, opening the diffuser behaves better with respect to the efficiency. Figure 3 shows the clear trend that opening the diffuser improves the efficiency performance when the rotational speed is decreased. At $N_{max}$, the highest peak efficiency of the five angles is the datum case. At a rotational speed of $0.8N_{max}$, the 'open 5°' case has the highest efficiency but, at a rotational speed of $0.4N_{max}$, the 'open 10°' case has the highest efficiency. The impeller and the diffuser of the datum case were designed to match well at the maximum rotational speed. As the rotational speed decreases, the diffuser throat required for good matching should be larger;[29] therefore, opening the diffuser improves the matching between the diffuser and the impeller and benefits the stage efficiency at low speeds. For a given operating point, there is an optimal angle for the diffuser vanes to achieve the highest efficiency. For instance, when the compressor operates at the point where the mass flow is 0.1 kg/s and the pressure ratio is 1.4, the efficiency of the open 5° case is 0.6% higher than that of the datum compressor. Therefore, the method of variable diffuser vanes is able not only to widen the operating range but also to improve the efficiency performance.

## Discussion on the range extension

In this section, several effects of the variable diffuser vanes, which are concerned with the choking flow, the surge flow and the efficiency, are discussed in detail.

*Assessment of the choking component.* When a duct is choked, the mass flow through the duct is kept at the maximum, its throat is in the sonic condition and the flow conditions upstream of the throat are not influenced by the outlet boundary.[30] For the compressor with a vaned diffuser, choke may occur at the diffuser or the impeller. The location of the critical section or sonic section depends on the rotational speed, the inlet conditions, the throats of the impeller and the diffuser and the blockage factor. At a rotational speed of $N_{max}$, the datum compressor must be choked at the diffuser. The evidence is that the open 5° case increases the choking flow from 0.515 kg/s to 0.517 kg/s. Although this increment is fairly small, it is definitely not caused by computation errors. The choking flow of the open 10° case is also 0.517 kg/s, which confirms that the value is not fortuitous. Furthermore, the consistency of the choking flows of the open 10° case and the open 5°

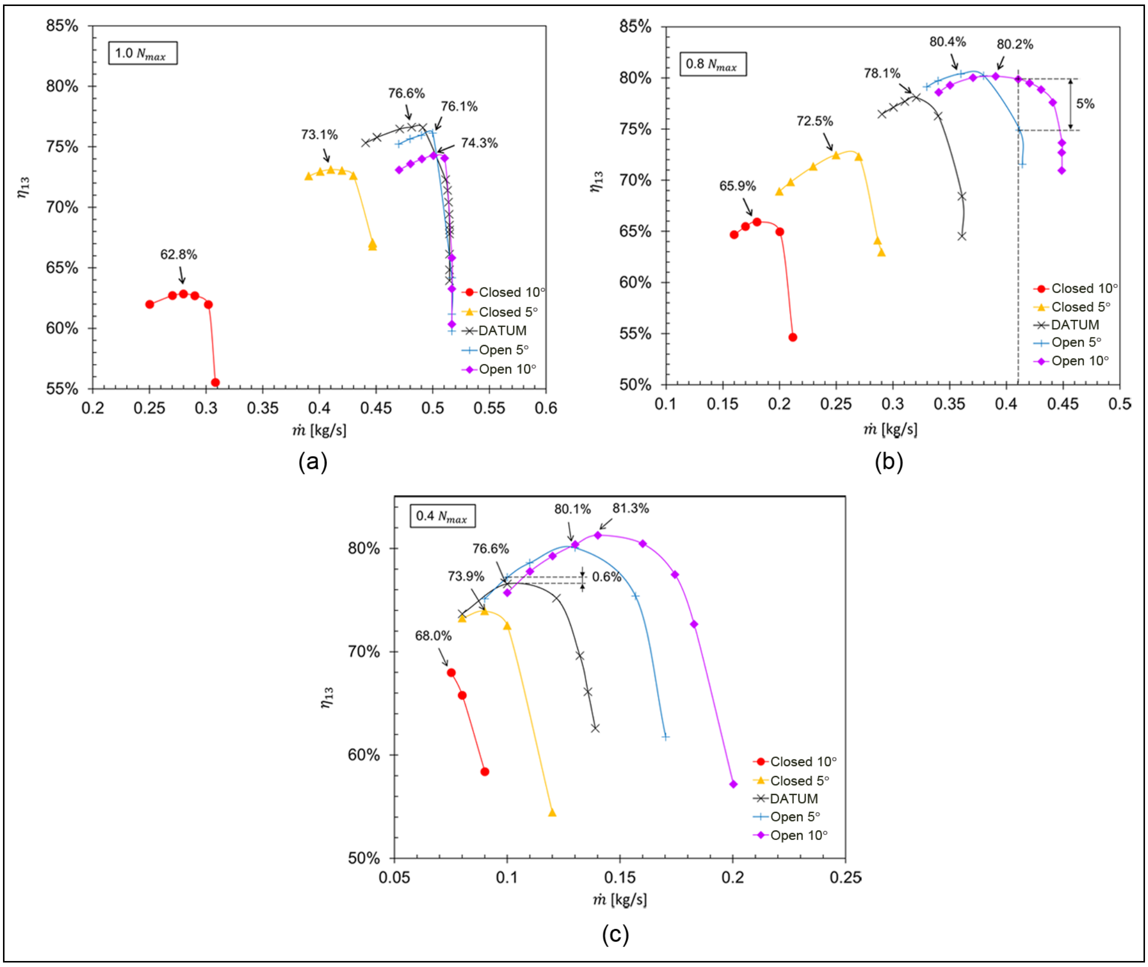


**Figure 3.** Efficiency performances for various rotational speeds: (a) $N_{max}$ (b) 0.8 $N_{max}$ (c) 0.4 $N_{max}$.

case implies that the diffuser no longer controls the choking flow of compressor after it opens by 5° and 10° (the throat areas of the diffusers are shown in Table 1; opening by 5° enlarges the diffuser throat greatly but only slightly increases the choking flow) and that the value of 0.517 must be the choking flow of the impeller at $N_{max}$ (the vaneless compressor was meshed and simulated, and its choking flow also proves to be 0.517 kg/s). Figure 4 shows a more specific proof for choking at the impeller. A and B are the choke points of the open 10° case at the maximum speed but with different outlet pressures. On the surface near the inducer, the static pressure distributions of A and B are almost the same. In contrast, the static pressure at the rotor–stator interface varies with the outlet pressure. Therefore, the critical section of choking must be located upstream of the interface, and the impeller must be the choke component for the open 10° case at $N_{max}$. By using the method in Figure 4, the choke component of a centrifugal compressor can be assessed. In fact, considering that the diffuser tends to control the choking flow at lower rotational speeds,[25,28] the choke components in many cases at low rotational speeds can be determined without observing the details of the flow fields. All the choking components for the different compressors and the different rotational speeds were assessed by observation of the flow field or just inference, as shown in Table 2. At rotational speeds lower than $N_{max}$, it is almost always the diffuser that is choked. Therefore, opening the diffuser shifts the choke line greatly, except at $N_{max}$.

*Highest efficiencies at different speeds.* Evaluation of the matching between the impeller and the diffuser is strongly associated with assessing the choking component. Therefore, on the basis of the previous discussion about the choke, the matching for a high efficiency and the matching for a low surge flow are discussed.

At $N_{max}$, it is the datum compressor that has the highest efficiency of all the five compressors. The main reason for this very high efficiency is the closeness of the impeller choking flow (0.517 kg/s) to the choking flow of the datum diffuser (0.515 kg/s). At a given rotational speed, the compressor which consist of components that both choke at the same mass flow usually has an excellent efficiency performance,[28] because the components match well in this condition. As shown in Figure 5(a), for the datum compressor, both the impeller and the diffuser operate with their best

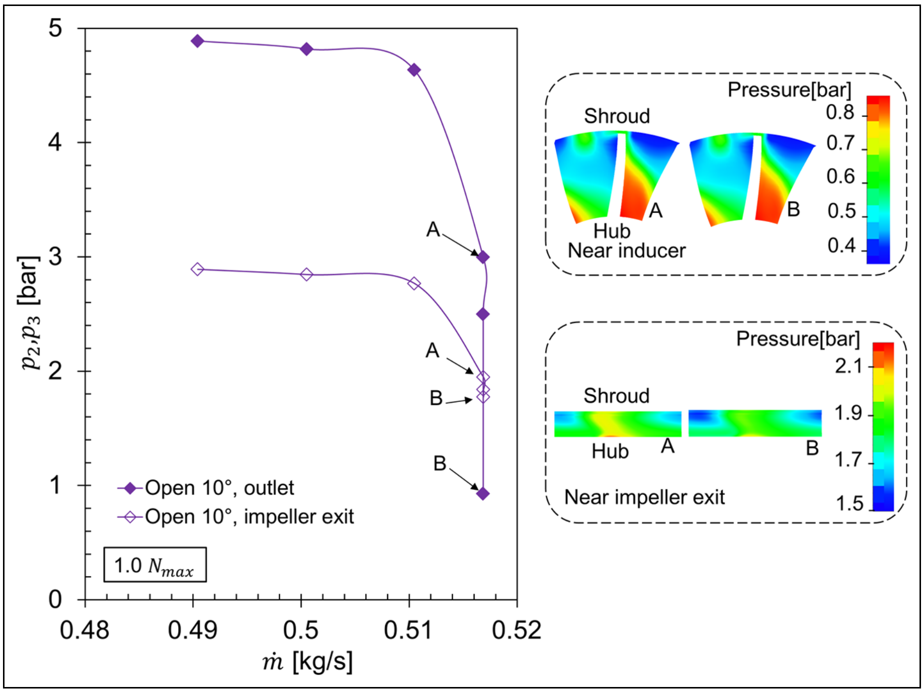


**Figure 4.** Static pressure characteristics of the open 10° case near the choke region at $N_{max}$.

**Table 2.** Choking components in various conditions.

| Rotational speed | Choking component for the following | | | | |
|---|---|---|---|---|---|
| | Closed 10° case | Closed 5° case | DATUM case | Open 5° case | Open 10° case |
| $N_{max}$ | Diffuser | Diffuser | Diffuser[a] | Impeller[a] | Impeller[a] |
| $0.9N_{max}$ | Diffuser | Diffuser | Diffuser | Diffuser[a] | Impeller[a] |
| $0.8N_{max}$ | Diffuser | Diffuser | Diffuser | Diffuser | Diffuser[a] |
| $0.6N_{max}$ | Diffuser | Diffuser | Diffuser | Diffuser | Diffuser |
| $0.4N_{max}$ | Diffuser | Diffuser | Diffuser | Diffuser | Diffuser |

[a]Obtained by observing the flow field (the others are obtained by inference).

performances at a mass flow rate near 0.48 kg/s where the peak stage efficiency is located. For each case with an open diffuser or a closed diffuser at $N_{max}$, a large difference between the choking flows of the components results in mismatching and a comparatively low efficiency. At rotational speeds of $0.8N_{max}$ or $0.4N_{max}$, the compressor with an open diffuser has an advantage with respect to the efficiency; this arises because opening the diffuser makes the choking flow of the diffuser approach that of the impeller. After opening the diffuser or improving the matching, the peak stage efficiency at low rotational speeds is even higher than that at $N_{max}$, because the impeller efficiencies at low rotational speeds are much higher than that at $N_{max}$. Figure 5 shows the impeller efficiencies and the diffuser loss coefficients at different rotational speeds. At each rotational speed, the impeller efficiency performances of the different cases have almost the same trend lines, which means that the impeller operates with good consistency even when different diffusers are used. It also validates the matching method employed by Tamaki et al.[31] where matching an impeller and different diffusers is based on only one impeller characteristic (they tested a compressor with a vaneless diffuser to obtain the impeller characteristic and assumed that the impeller characteristic does not change when mounted with different vaned diffusers). At each rotatonal speed, the impeller in the case that has the highest peak efficiency is always matched in its high-efficiency region. The reason is that the compressor which matches the choking flows well works efficiently. The impeller tends to be choked at high rotational speeds, so it can be deduced that, at a rotational speed even above $N_{max}$, the highest peak efficiency occurs in the compressor with a closed diffuser if the diffuser loss coefficient does not deteriorate too much.

Adjusting the diffuser vane angles not only changes the matching relation between the diffuser and the impeller but also influences the diffuser characteristics. At a rotational speed of $0.8N_{max}$, the diffuser loss

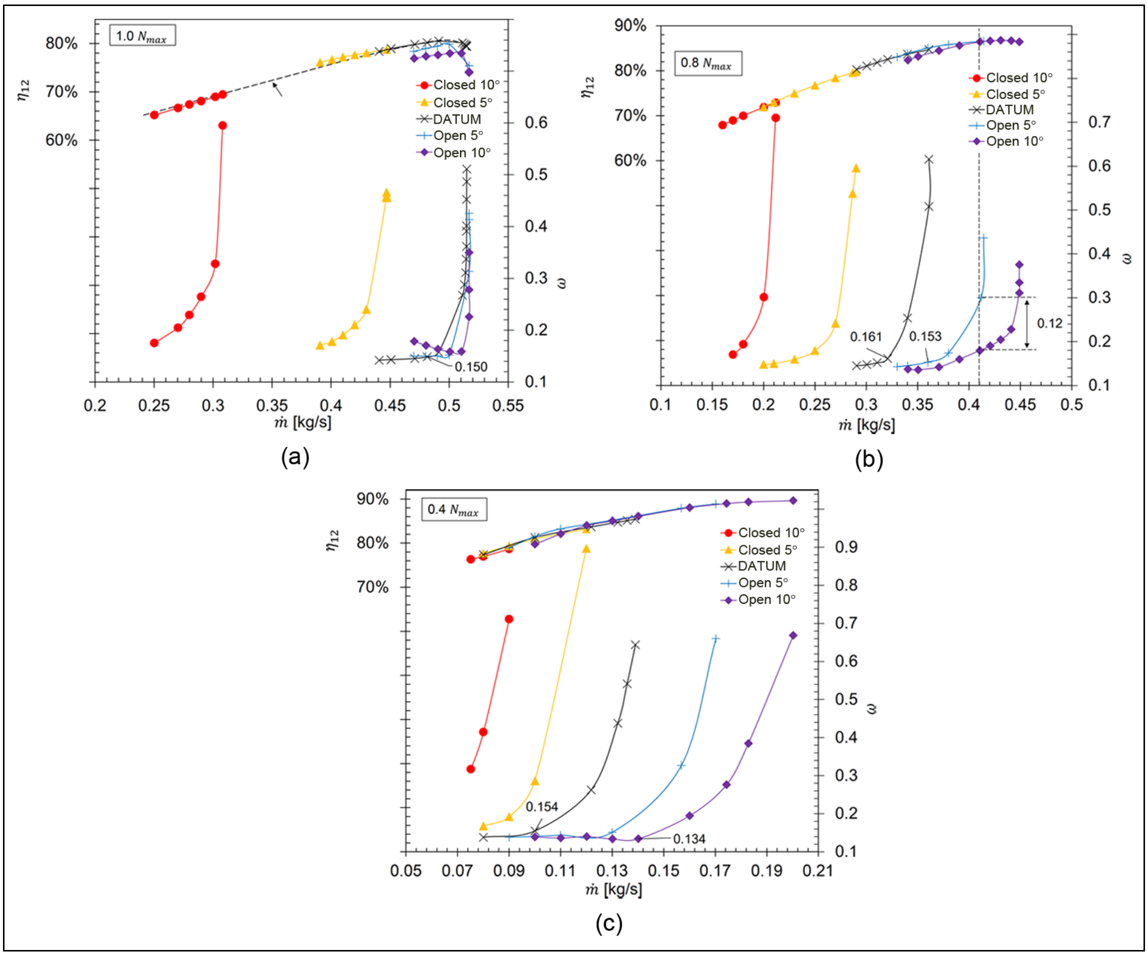


**Figure 5.** Adiabatic efficiency and diffuser loss coefficient performances of the impeller at the following rotational speeds (computed using the gas-state parameters at the inlet, the rotor–stator interface and the outlet): (a) $N_{max}$ (b) 0.8 $N_{max}$ (c) 0.4 $N_{max}$.

coefficient of the peak stage efficiency of the open 5° case is 0.153; this is slightly lower than that of the datum case, which is 0.161. The diffuser loss coefficient also decreases from 0.154 to 0.134 after opening the diffuser by 10° at $0.4N_{max}$. Therefore, at rotational speeds of $0.8N_{max}$ and $0.4N_{max}$, opening the diffuser improves its performance, which also contributes to a gain in the stage efficiency. However, in comparison with the change in the matching relation, the improvement in the diffuser performance has less impact on increasing the stage efficiency, since the reductions in the diffuser loss coefficient which are $0.161 - 0.153 = 0.008$ at $0.8N_{max}$ and $0.154 - 0.134 = 0.02$ at $0.4N_{max}$ are too slight. It should be noted that the diffuser loss coefficient of the 'closed 10°' case at a rotational speed of $0.4N_{max}$ changes greatly in comparison with that of the datum case. The compressor involved in surge before the diffuser reaches its lowest loss coefficient and we cannot even obtain a complete diffuser characteristic in this scenario; therefore, this case is not considered. An example is shown to evaluate the impact of the diffuser loss coefficient on the stage efficiency. The open 10° case and the open 5° case have the same impeller efficiencies at $0.8N_{max}$ and the mass flow rate of 0.41. However, the stage efficiency of the open 10° case is 5% higher than that of the open 5° case, since its diffuser loss coefficient is lower than that of the open 5° case by 0.12. If the impact of the diffuser loss coefficient is considered to be approximately linear, thus the decrease of 0.008 in the diffuser loss coefficient of the open 5° case at $0.8N_{max}$ can contribute to increasing the peak stage efficiency by $0.008 \times 5\%/0.12 \approx 0.33\%$, and the decrease of 0.02 in the diffuser loss coefficient of the open 10° case at $0.4N_{max}$ can have an impact of $0.02 \times 5\%/0.12 \approx 0.83\%$. However, the peak stage efficiency gained in the open 5° case at $0.8N_{max}$ is $80.4\% - 78.1\% = 2.3\%$, and the peak stage efficiency gained in the open 10° case at $0.4N_{max}$ is $81.3\% - 76.6\% = 4.7\%$. The impact of the change in the diffuser characteristic on the peak stage efficiency does exist, but it has less influence than the change in the matching relation.

*Closing the diffuser for low surge flow.* In order to obtain an excellent efficiency performance, the components can be matched by keeping them choked at the same mass flow. However, this matching may have to be abandoned if the operating flow range is insufficient. As shown in Figure 2, closing the diffuser shifts the surge lines at the expense of a decrease in the efficiency but contributes greatly to range extension. Therefore, if the method of variable diffuser vanes is employed, the diffuser can be closed to ensure that the compressor operates stably at extremely low mass flows and supports the engine to output a satisfactory low-end torque. This is the matching used for low surge mass flows in this paper.

Closing the diffuser makes the surge flow of the compressor lower at rotational speeds above $0.8N_{max}$, as shown in Figure 2. From Figure 5(a) and (b), it can be seen that the closed diffuser does not affect the characteristics of the impeller and only drives the impeller to operate in a lower-mass-flow-rate region. For instance, at the rotational speed of $0.8N_{max}$, the surge flow of the datum compressor is 0.29 kg/s. After closing the diffuser by 5°, the characteristics of diffuser seem to move towards the low-mass-flow-rate region and the impeller is able to operate at a mass flow rate of 0.2 kg/s. The flow stability in the impeller becomes worse when it operates in a lower-mass-flow-rate region. Comparatively, the flow stability in the diffuser contributes more to stabilizing the performance of the stage.

The slopes of the characteristics of the components of a centrifugal compressor have been used to assess the flow stability of the whole stage.[19, 32] As can be seen from

$$\frac{\partial \pi_{13}}{\partial \dot{m}} = \pi_{12}\frac{\partial \pi_{23}}{\partial \dot{m}} + \pi_{23}\frac{\partial \pi_{12}}{\partial \dot{m}} \tag{2}$$

a positive $\partial \pi_{13}/\partial \dot{m}$ indicates that the stage is potentially unstable; this can be caused by the positive slopes of the characteristics of the diffuser and the impeller. The slope $\partial \pi_{12}/\partial \dot{m}$ of the impeller characteristics and the slope $\partial \pi_{23}/\partial \dot{m}$ of the diffuser characteristics at the surge points of almost all speeds and all compressors are plotted in Figure 6 (the slopes at the surge point of the closed 10° case at $0.4N_{max}$ were abandoned since they deviated too much). Figure 6, which indicates the diffuser types, shows the trends that the impeller operates more unstably and the diffuser operates more stably in the compressor which has a closed diffuser. For the compressor with an open diffuser, the impeller tends to be more stable and the diffuser is potentially involved in instability. Because at some surge points the slopes $\partial \pi_{13}/\partial \dot{m}$ of the stage performance of the total compressor are not exactly near to zero, therefore, the slopes of the impeller characteristics and the slopes of the diffuser characteristics at the points in the dashed rectangle have the same signs.

However, at rotational speeds of $0.4N_{max}$ and $0.6N_{max}$, closing the diffuser has almost no influence on surge flow. The reason is that, at low rotational speeds, surge may be triggered and dominated by flow instability in the impeller and, in particularly, by flow instability in the inducer. Figure 7(a) shows the surge lines of the datum case and the closed 10° case. Closing the

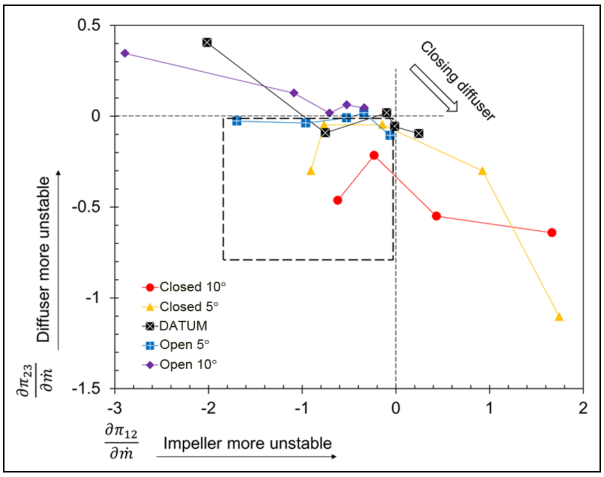


**Figure 6.** Slopes of the impeller and the diffuser performances at the surge points.

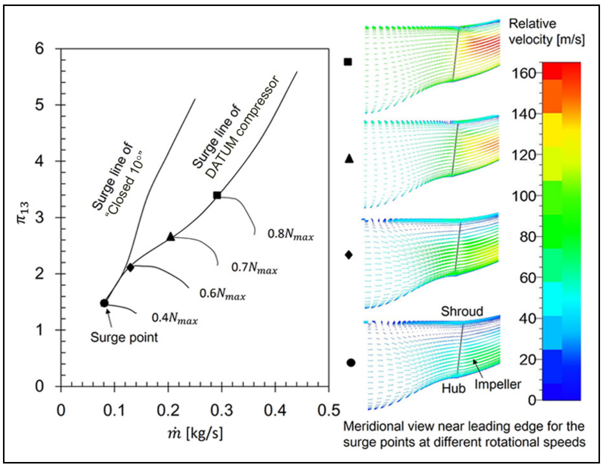


**Figure 7.** Relative velocity near the inducer at the surge points for different rotational speeds.

diffuser does not reduce the surge flows at $0.4N_{max}$ and $0.6N_{max}$. The surge points of the datum case are labelled in the figure. The meridional views of the relative velocity near the leading edge of the impeller at those points are shown in Figure 7(b). At the surge points of $0.4N_{max}$ (indicated by a full circle) and $0.6N_{max}$ (indicated by a full diamond), violent flow separation and recirculation occur near the tip of the leading edge, which indicates that the impeller is involved in great flow instability. However, for the surge points at higher rotational speeds, there is no such feature of flow instability in the impeller, which means that the impeller operates stably when the compressor is involved in surge. Therefore, at low rotational speeds of $0.4N_{max}$ and $0.6N_{max}$ where surge is triggered by the impeller, adjustment of the diffuser cannot contribute to reducing the surge flow. In contrast, at high rotational speeds, surge is induced by the diffuser, thus closing the diffuser vanes decreases the surge flow considerably.

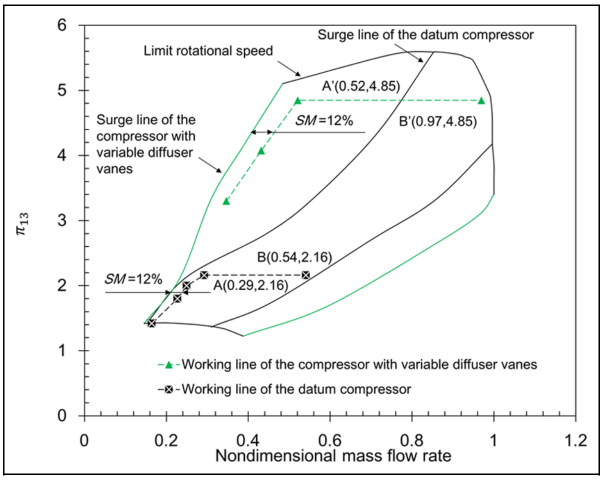


**Figure 8.** Operating points of the compressor where the surge margin equals 12% for the DATUM compressor and the compressor with variable diffuser vanes.
*SM*: surge margin.

## Improving the low-end torque of an engine

The operating range of the compressor was extended by the method of variable diffuser vanes, which benefits the low-end torque performance of engine. The method of variable diffuser vanes facilitates the compressor to provide an intake at a high pressure by extending the operating range. To be specific, an engine can deliver a high torque at a low engine shaft speed, because the compressor is able to provide a high pressure ratio at extremely low mass flow rates. This is explained as follows.

The datum compressor was scaled to match the engine. As shown by the working line of the datum compressor in Figure 8, the compressor was matched at a pressure ratio of 2.16. Point A is the working condition of the maximum torque and point B is the working condition of full power. The maximum torque speed is 54% of the rated speed. The surge margin of the compressor which is defined as

$$\text{Surge margin} = \left(1 - \frac{\dot{m}_s}{\dot{m}_w}\right)_{\pi\,=\,constant} \times 100\% \quad (3)$$

is controlled to be above 12% in this paper. To make use of the surge margin fully in order to improve the torque performance, the working line of the compressor goes along the line where the surge margin equals 12%. After employing variable diffuser vanes, the operating range of the compressor was extended greatly; consequently, its working line also changes.

At a given pressure ratio of the compressor, the shaft speed of the engine should be almost proportional to the mass flow of air through the compressor according to

$$\text{Engine shaft speed} = \frac{2\dot{m}}{\eta_v \rho_{in} V} \propto \frac{\dot{m}}{\rho_{in}} \quad (4)$$

$$\rho_{in} \approx \rho_{t3} \propto \pi_{13}^{1/\gamma} \quad (5)$$

In equation (5), the flow from the compressor inlet to the cylinder is assumed to be isentropic, and so the air density entering the cylinder does not change if the pressure ratio delivered by compressor remains the same. Therefore, the ratio of the mass flow at the maximum torque point to the mass flow at full power should be the same as the ratio of the maximum torque speed to the rated speed. If the surge flow is not sufficiently small, the maximum torque speed of the engine may not be sufficiently low or the low-end torque can deteriorate. With variable diffuser vanes, the compressor has a broader operating range at a high pressure ratio; therefore, the compressor can be matched at a high pressure ratio and operates stably at the maximum torque point with a sufficiently low engine shaft speed. The working line of the compressor can move upwards on the map with variable diffuser vanes. Limited by the rotational speed of the compressor, the pressure ratio of working line can move only up to 4.85. Still, the working line in Figure 8 satisfies the surge margin requirement. Also, $\dot{m}_{A'}/\dot{m}_{B'} = 0.54$, which guarantees that the engine equipped with variable diffuser vanes is able to achieve the required maximum torque speed. If the working line moves higher, the ratio of the mass flow rates at these two points must be larger than 0.54 and the maximum torque speed increases, which fails to satisfy the torque performance. According to the relationship

$$\begin{aligned}\text{Engine torque output} &= \frac{\text{engine power output}}{\text{engine shaft rotational speed}} \\ &= \frac{\eta_e \dot{m} H_u}{\alpha \times \text{engine shaft rotational speed}} \\ &\propto \rho_{in}\end{aligned} \quad (6)$$

the engine torque output is proportional to the air density entering the cylinder, which is related to the pressure ratio. Therefore, the ratio of the engine torque at point A′ to the engine torque at point A is $(4.85/2.16)^{1/1.4} = 1.78$. Thus, the maximum torque of engine can be improved by 78%.

In the estimation, the changes in the volumetric efficiency $\eta_v$, the effective efficiency $\eta_e$ and the air-to-fuel ratio $\alpha$ are not taken into account, and so this is quite a rough estimation. The matching of the turbine is also an important issue, and the question of whether the turbine can support the compressor to operate in a wide flow range still has not been resolved. In order to predict the improvement precisely, more work on one-dimensional engine simulations is necessary.

## Conclusions and remarks

In order to widen the operating range of a compressor and to improve the torque performance of an engine, the method of variable diffuser vanes was employed.

This study exploited numerical simulations to investigate the performances of centrifugal compressors with diffuser vane angles varying from $-10°$ to $10°$. The potential of variable diffuser vanes for extending the operating range of a compressor was evaluated. The improvement in the torque obtained by using variable diffuser vanes was also estimated. Some conclusions are drawn as follows.

1. The method of variable diffuser vanes with angles between $-10°$ and $10°$ has the potential to improve the operating range by 23.5–54.9% at the pressure ratio of 4.8 (this high pressure ratio may be the preferred choice for future turbocharged engines). At high rotational speeds where the choking flow of impeller is near to that of the diffuser, movement of the surge line towards a low mass flow rate which is contributed by closing the diffuser is the main reason for the range extension. Near low rotational speeds or low pressure ratios, the choke line moves significantly on opening the diffuser, which extends the operating range as the main contributor. At medium rotational speeds, shifts in both the choke line and the surge line are significant. By adjusting the diffuser vane angles, the impeller and the diffuser can be matched to provide a high efficiency performance or a low surge flow.
2. At a rotational speed of $0.8N_{max}$ and above, the surge flow decreases on closing the diffuser. Closing the diffuser with a smaller throat area drives the impeller to operate in the region of lower mass flow rates. The flow stability in the impeller becomes worse, because it operates in a lower-mass-flow-rate region. Comparatively, the flow stability in the closed diffuser becomes better and contributes more to stabilizing the stage performance near surge. At rotational speeds of $0.6N_{max}$ and $0.4N_{max}$, closing the diffuser fails to reduce the surge flow, because surge is dominated by the flow instability in the inducer which arises owing to the violent recirculation near the inducer tip.
3. In this design, at the rotational speed of $N_{max}$ where the choking mass flow of the diffuser is near to that of the impeller, opening the diffuser fails to increase significantly the choking mass flow of the stage, because choke may occur in the impeller after opening the diffuser. In contrast, opening the diffuser extends the operating range greatly at low speeds, because the stage is choked at the diffuser at these speeds. A method to assess the choking component of a centrifugal compressor is proposed. If the diffuser is choked, the flow field upstream of the diffuser does not vary with the back pressure. If the impeller is choked, the flow field in the diffuser will be influenced by the change in the back pressure.
4. After employing variable diffuser vanes, the engine is able to deliver a high torque output at a low shaft speed. Because the operating range of the compressor is extended by using variable diffuser vanes between $-10°$ and $10°$, this improves the maximum torque by 78%, and so the low-end torque performance is also improved greatly. The method of variable diffuser vanes also provides the potential for further downsizing, because the compressor is able to deliver a high pressure ratio stably in wide operating range.
5. The mechanical structure and the control system for adjusting the diffuser vanes increase the production cost and the maintenance fee, which are not cheap for a common turbocharger. As far as the authors know, the method of variable diffuser vanes has only been widely adopted for industrial centrifugal compressors. Currently, turbocharger compressors in passenger vehicles are not required to deliver a high pressure ratio frequently, so it is not worthwhile to have variable diffuser vanes in a common turbocharger. This is only necessary for some special cases such as heavy-load diesel engines and high-altitude work environment. In those occasions, compressors often operate with a high pressure ratio, so variable diffuser vanes may be competitive in the market. The cost will not be a problem if there is an extensive demand. A trend of turbocharging is to deliver high-pressure-ratio intake and to downsize engines. With this trend, variable diffuser vanes must be a preferred choice in the future when high pressure ratios will be widely applied to passenger vehicles.
6. The more complicated structure and real-time control of the diffuser cause the reliability of the turbocharger compressor to deteriorate. However, when it is considered that those turbochargers which are equipped with variable geometry turbo are able to work for a long time, the increase in the complexity of the compressor may not be a serious obstacle for reliability.

## Declaration of conflicting interests

The author(s) declared no potential conflicts of interest with respect to the research, authorship, and/or publication of this article.

## Funding

The author(s) disclosed receipt of the following financial support for the research, authorship, and/or publication of this article: This research was supported by the National Natural Science Foundation of China (grant number 51176087).

## References

1. Kalghatgi GT. Developments in internal combustion engines and implications for combustion science and future transport fuels. *Proc Combust Inst* 2015; 35: 101–115.
2. Aoyagi Y, Kunishima E, Asaumi Y et al. Diesel combustion and emission using high boost and high injection

pressure in a single cylinder engine. *JSME Int J, Ser B* 2005; 48: 648–655.
3. Aoyagi Y, Yamaguchi T, Osada H et al. Improvement of thermal efficiency of a high-boosted diesel engine with focus on peak cylinder pressure. *Int J Engine Res* 2011; 12: 227–237.
4. Wakisaka Y, Hotta Y, Inayoshi M et al. Emissions reduction potential of extremely high boost and high EGR rate for an HSDI diesel engine and the reduction mechanisms of exhaust Emissions. SAE paper 2008-01-1189, 2008.
5. Friedl H, Certic M, Fuerhapter A et al. Technology features and development methods for spark ignited powertrain to meet 2020 $CO_2$ emission targets. SAE paper 2013-36-0438, 2013.
6. Turner JWG, Pearson RJ and Kenchington SA. Concepts for improved fuel economy from gasoline engines. *Int J Engine Res* 2005; 6(2): 137–157.
7. Blair J and Bower G. Development of a Miller cycle powersports engine. SAE paper 2014-32-0090, 2014.
8. Bandivadekar A, Bodek K, Cheah L et al. On the road in 2035: reducing transportation's petroleum consumption and GHG emissions. Report LFEE 2008-05 RP, Laboratory for Energy and the Environment, Massachusetts Institute of Technology, Cambrdige, Massachusetts, USA, 2008 July, http://web.mit.edu/sloan-auto-lab/research/beforeh2/otr2035/ (2008, accessed 24 December 2015).
9. Taylor AMKP. Science review of internal combustion engines. *Energy Policy* 2008; 36: 4657–4667.
10. Galindo J, Serrano JR, Climent H et al. Experiments and modelling of surge in small centrifugal compressor for automotive engines. *Expl Thermal Fluid Sci* 2008; 32: 818–826.
11. Wöhr M, Chebli E, Müller M et al. Development of a turbocharger compressor with variable geometry for heavy-duty engines. *Int J Engine Res* 2015; 16(1): 23–30.
12. Ricardo MB, Apostolos P and Yang MY. Overview of boosting options for future downsized engines. *Sci China Ser E* 2011; 54: 318–331.
13. Zheng X, Zhang Y, Yang M et al. Stability improvement of high-pressure-ratio turbocharger centrifugal compressor by asymmetrical flow control – Part II: nonaxisymmetrical self-recirculation casing treatment. *Trans ASME, J Turbomach* 2012; 135: 021007.
14. Yang M, Zheng X, Zhang Y et al. Stability improvement of high-pressure-ratio turbocharger centrifugal compressor by asymmetric flow control – Part I: non-axisymmetrical flow in centrifugal compressor. *Trans ASME, J Turbomach* 2012; 135: 021006.
15. Rodgers C and Brown D. A performance autopsy of three centrifugal compressors for a small gas turbine. In: *ASME turbo expo 2010: power for land, sea, and air*, Glasgow, UK, 14–18 June 2010, paper GT2010-22037, pp. 239–247. New York: ASME.
16. Swain D. *Impact of impeller blade trimming on the performance of centrifugal compressors*. PhD Thesis, Michigan State University, East Lansing, Michigan, USA, 2014.
17. Whitfield A. Review of variable geometry techniques applied to enhance the performance of centrifugal compressors. In: *15th international compressor engineering conference*, West Lafayette, Indiana, USA, 25–28 July 2000, paper 1368, pp. 63–70. West Lafayette, Indiana: Purdue University Press.
18. Simon H, Wallmann T and Monk T. Improvements in performance characteristics of single-stage and multistage centrifugal compressors by simultaneous adjustments of inlet guide vanes and diffuser vanes. *Trans ASME, J Turbomach* 1987; 109: 41–47.
19. Hunziker R and Gyarmathy G. The operational stability of a centrifugal compressor and its dependence on the characteristics of the subcomponents. *Trans ASME, J Turbomach* 1994; 116: 250–259.
20. Jiao K, Sun H, Li X, Wu H et al. Numerical investigation of the influence of variable diffuser vane angles on the performance of a centrifugal compressor. *Proc IMechE Part D: J Automobile Engineering* 2009; 223(8): 1061–1070.
21. Zheng X, Huang Q and Liu A. Loss mechanisms and flow control for improved efficiency of a centrifugal compressor at high inlet prewhirl. *Trans ASME, J Turbomach* 2016; 138: 101011.
22. Guo Z, Song L, Zhou Z et al. Multi-objective aerodynamic optimization design and data mining of a high pressure ratio centrifugal impeller. *Trans ASME, J Engng Gas Turbines Power* 2015; 137(9): 092602.
23. Zheng X, Huenteler J, Yang M et al. Influence of the volute on the flow in a centrifugal compressor of a high-pressure ratio turbocharger. *Proc IMechE Part A: J Power and Energy* 2010; 224: 1157–1169.
24. *FINE™/Turbo user manual, v8.7*. Brussels: Numeca, 2010.
25. Cumpsty NA. *Compressor aerodynamics*. Malabar, Florida: Krieger, 2004, pp. 288, 364.
26. Baines NC. *Fundamentals of turbocharging*. White River Junction, Vermont: Concepts NREC, 2005, pp. 3, 66.
27. Ubben S and Niehuis R. Experimental investigation of the diffuser vane clearance effect in a centrifugal compressor stage with adjustable diffuser geometry – Part I: compressor performance analysis. *Trans ASME, J Turbomach* 2014; 137: 031003.
28. Zheng X and Huang Q. Potential of the range extension of compressors with a variable inlet prewhirl for automotive turbocharged engines with an ultra-high-power density. *Proc IMechE Part D: J Automobile Engineering 015*; 229(14): 1959–1968.
29. Casey M and Rusch D. The matching of a vaned diffuser with a radial compressor impeller and its effect on the stage performance. *Trans ASME, J Turbomach* 2014; 136: 121004.
30. White F. *Fluid mechanics*. New York: McGraw-Hill, 2008, p. 617.
31. Tamaki H, Nakao H and Saito M. The experimental study of matching between centrifugal compressor impeller and diffuser. *Trans ASME, J Turbomach* 1999; 121(1): 113–118.
32. Dean RC. The fluid dynamic design of advanced centrifugal compressors. Lecture notes, Von Karman Institute, Brussels, Belgium, 1974.

## Appendix 1

### *Notation*

| | |
|---|---|
| $H_u$ | fuel heat value |
| $\dot{m}$ | mass flow rate |
| $\dot{m}_c$ | choke mass flow rate |
| $\dot{m}_s$ | surge mass flow rate |

| | |
|---|---|
| $\dot{m}_w$ | mass flow rate at the working point of the compressor mounted on the engine |
| $N_{max}$ | maximum rotational speed of the compressor |
| $p_{t1}$ | total pressure at the inlet |
| $p_{t2}$ | total pressure at the rotor–stator interface (the impeller exit or the diffuser inlet) |
| $p_{t3}$ | total pressure at the outlet |
| $p_1$ | static pressure at the inlet |
| $p_2$ | static pressure at the rotor–stator interface (the impeller exit or the diffuser inlet) |
| $p_3$ | static pressure at the outlet |
| $T_{t1}$ | average temperature at the inlet |
| $T_{t3}$ | average temperature at the outlet |
| $V$ | volume of the engine |
| $\alpha$ | air-to-fuel ratio |
| $\gamma$ | specific heat ratio = 1.4 (constant) for air in this paper |
| $\eta$ | isentropic efficiency |
| $\eta_e$ | effective isentropic efficiency of the engine |
| $\eta_v$ | volumetric isentropic efficiency |
| $\eta_{12}$ | adiabatic efficiency of the impeller |
| $\eta_{13}$ | adiabatic efficiency of the whole compressor calculated from the inlet to the outlet $= T_{t1}\left(\pi_{13}^{(\gamma-1)/\gamma} - 1\right)/(T_{t3} - T_{t1})$ |
| $\pi$ | total pressure ratio |
| $\pi_{13}$ | ratio of the total pressure at the outlet to the total pressure at the inlet $= p_{t3}/p_{t1}$ |
| $\pi_{23}$ | ratio of the total pressure at the outlet to the total pressure at the rotor–stator interface (the impeller exit or the diffuser outlet) $= p_{t3}/p_{t2}$ |
| $\rho_{in}$ | density of the air in the engine cylinder |
| $\omega$ | diffuser loss coefficient $= (p_{t2}-p_{t3})/(p_{t2}-p_2)$ |

## Subscripts

| | |
|---|---|
| $c$ | choke |
| $d$ | diffuser |
| $i$ | impeller |
| $in$ | cylinder inlet |
| $max$ | maximum |
| $s$ | surge |
| $t$ | total or stagnation parameter |
| $w$ | working point of the compressor mounted on the engine |
| 1 | inlet |
| 2 | rotor–stator interface (the impeller exit or the diffuser inlet) |
| 3 | outlet |